Mossbauer Spectroscopy of ^{57}Fe

Shawn Westerdale*
MIT Department of Physics
(Dated: May 13, 2010)

Mossbauer spectroscopy is a high-precision method of probing the hyperfine structure of an atom by pulsing it with x-rays under small doppler shifts. Using this method, we were able to measure the ground and excited state Zeeman energy gaps, isomer shift, quadrupole splittings, nuclear magnetic field, and ground state to excited state magnetic moment ratio of ^{57}Fe in various chemical environments, as shown in table I. Specifically, we examined these effects in enriched metallic ^{57}Fe, Fe_2O_3, Fe_3O_4, $FeSO_4$, and $Fe_2(SO_4)_3$. We found that most of our measurements agreed with previously published values to good accuracy. We also measured the natural linewidth of ^{57}Fe to 14.4 keV photons to be $8.60 \times 10^{-9} \pm 1.34 \times 10^{-9}$ eV. By controlling the temperature of the sample, we were also able to observe the effects of relativistic time dilation and measure the temperature coefficient of the thermal resonance shift $\frac{\Delta E}{E}$ to be $-1.9 \pm 0.3 \times 10^{-15}$ °C^{-1}.

I. INTRODUCTION

I.1. Mossbauer Spectroscopy

To see how Mossbauer spectroscopy works, it is instructive to look at the specific case involving ^{57}Fe. ^{57}Fe has an excited state ^{57m}Fe that occupies an energy level 14.4 keV above the ground state. To see how hyperfine and chemical interactions affect the structure of the ^{57}Fe energy levels, we can use the decay of ^{57m}Fe. When ^{57m}Fe decays, it releases a 14.4 keV photon.

In theory, the ^{57}Fe atom would absorb an incident photon and transition up into the excited state. However, in practice this does not happen. If we consider the kinetic energy of the ^{57m}Fe nucleus, we find that $E_{recoil} = \frac{p_\gamma^2}{2m_{Fe}}$. Since the energy of a photon is equal to the speed of light times its momentum, we can conclude that

$$E_{recoil} = \frac{(14.4keV)^2}{2m_{Fe}c^2} \tag{1}$$

A free iron nucleus will therefore redshift the photon it emits. Similarly, we find that a free iron nucleus absorbing the photon would recoil by the same amount, further redshifting the photon. The total recoil energy is on the order of 0.004eV, meaning that all hyperfine resolution, which tends to be on the order of 10^{-10} eV, is lost.

Before Mossbauer's innovation, this was a large problem for precision atomic physicists. Most spectroscopic techniques of this sort used a gases for the source and the absorber, and so these nuclear recoils prevented physicists from probing the hyperfine structure.

Mossbauer's innovation was to use solids instead of gases. For the case of iron spectroscopy, if we embed the ^{57m}Fe source atoms and the receiving ^{57} atoms in large crystals, the lattices increase the total masses, and reduce the total recoil. This can be seen in equation (1), which predicts that the recoil is inversely proportional to the mass of the source or receiver. For example, a crystal structure with mass 10^{-6}g only recoils with approximately 1.85×10^{-19} eV, and so we can still resolve the hyperfine structure.

Mossbauer spectroscopy makes use of this effect by slowly moving the source, allowing small doppler shifts in the emitted photon to shift the photon's energy on small enough scales to resolve the atoms hyperfine structure.

II. SMALL PERTURBATIONS OF THE ATOMIC HAMILTONIAN

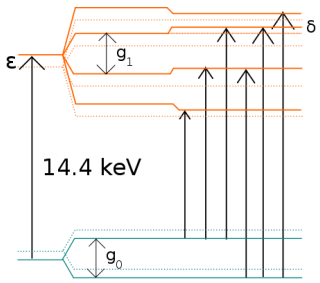

FIG. 1. A diagram of the different perturbations to the 14.4 keV energy gap, showing the isomer shift ϵ, the quadrupole splitting δ, and the Zeeman splitting g_0 and g_1

II.1. Hyperfine Zeeman Splitting

Since iron has an unpaired electron in the 1S orbital, the movement of the electron around the nucleus generates a strong magnetic field, akin to the magnetic field generated by a current in a loop. Since the electron is moving near the speed of light in circles of radii on the order of an angstrom, we expect this magnetic field to be very strong.

This strong magnetic field can split the energy levels of the atom according to their total angular momenta by the relation $\mathcal{H}' = \vec{\mu} \cdot \vec{B}$, where $\vec{B}$ is the magnetic field and $\vec{\mu}$

*shawest@mit.edu

is the magnetic moment of the atom. The magnetic moment depends on the spin of the transitioning electrons, the transitioning electron's orbital angular momentum, and the total nuclear angular momentum. We call the vector $\vec{F}$ the total angular momentum and is the sum of these three angular momenta terms and find that we can express the energy shift due to the magnetic field as

$$\mathcal{H}' = g_L m_F \mu_N B \tag{2}$$

where g_L is the nuclear Landé g-factor—a numerical factor the depends on the interactions of the three angular momenta and results from their relative angles and their magnitudes—m_F is the magnitude of the projection of $\vec{F}$ along the direction of $\vec{B}$ and ranges from f to $-f$ in discrete intervals of 1, where the eigenvalues of $\vec{F}^2 = f(f+1)$. For ^{57}Fe, we find that $f = \frac{1}{2}$ for the ground state and $f = \frac{3}{2}$ for the first excited state, leading to the six different energy levels we see in figure 1.

We also define constants g_0 and g_1 to be the energy gaps between these hyperfine energy levels.

II.2. Isomer Shift

The electron density at the nucleus can have a small effect on the energy levels of the atom. Since the electron density is a function of the electron radius, and when the atom absorbs the 14.4 keV photon, the electron radius increases slightly, we find there is a small shift in the ground state and first excited state energy levels. In particular, the ground state energy level decreases by a small amount and the first excited state similarly increases by a little.

As a result, the energy of the photon that actually resonates with the 14.4 keV transition is slightly more than 14.4 keV. This observed shift appears as an overall shift of the center of gravity of the distribution, so that that the resonant peaks appear to be centered around an energy level other than 0 eV. We call this energy shift ϵ, the isomer shift, and is the sum of the shift of the ground state energy and the first excited state energy levels.

II.3. Quadrupole Splitting

If the atom of interest is chemically interacting with other atoms, its electron orbitals may be somewhat distorted. This can cause an uneven electric field distribution around the nucleus known as the quadrupole moment, denoted by e^2Q. This quadrupole moment splits the energy levels by δ, according to

$$\delta = \frac{qe^2Q}{4I(2I-1)}[3m_F^2 - I(I+1)] \tag{3}$$

where q is the gradient of the electric field at the nucleus and I is the spin of the nucleus. This quadrupole interaction only affects the excited state of the atom. For ^{57}Fe, we find that the $m_F = \pm\frac{3}{2}$ and $m_F = \pm\frac{1}{2}$ states have equal magnitude but opposite sign, leading to the small splittings of δ shown in figure 1.

II.4. Total Perturbations

If we consider all three of the aforementioned interactions, we can see that the transitions depicted in figure 1 all have energies described by

$$\begin{aligned}
\Delta\mathcal{H}' &= (\frac{3}{2}g_L - \frac{1}{2}g_L')\mu_N B + \epsilon - \delta \\
\Delta\mathcal{H}' &= (\frac{1}{2}g_L - \frac{1}{2}g_L')\mu_N B + \epsilon + \delta \\
\Delta\mathcal{H}' &= (-\frac{1}{2}g_L - \frac{1}{2}g_L')\mu_N B + \epsilon + \delta \\
\Delta\mathcal{H}' &= (\frac{1}{2}g_L + \frac{1}{2}g_L')\mu_N B + \epsilon + \delta \\
\Delta\mathcal{H}' &= (-\frac{1}{2}g_L + \frac{1}{2}g_L')\mu_N B + \epsilon + \delta \\
\Delta\mathcal{H}' &= (-\frac{3}{2}g_L + \frac{1}{2}g_L')\mu_N B + \epsilon - \delta
\end{aligned}$$

where g_L' denotes the nuclear Landé g-factor of the excited state. Since this system is overconstrained, if we measure the absorption energies of the different hyperfine energy levels, we can take linear combinations of the different $\Delta\mathcal{H}'$ to obtain values for all of the splitting terms.

III. NATURAL LINE WIDTH

The Heisenberg uncertainty principle $\Delta E \Delta t \geq \frac{\hbar}{2}$ suggests that for some characteristic time t, the minimum width of the energy absorption line would be $\Delta E = \frac{\hbar}{2t}$. If we call this energy spread the natural line width of the decay, denoted by Γ_n, we can relate it to the half life τ of the ^{57m}Fe to ^{57}Fe decay by $\Gamma_n = \frac{\hbar \ln 2}{\tau}$. We can measure this Γ_n by measuring the full width at half maximum of the absorption peak of a ^{57}Fe-rich absorber at a range of thicknesses and extrapolating the line width down to an absorber of zero thickness. We expect to find that this thickness is related to the half life of the excited state decay.

IV. TIME DILATION AND THE TEMPERATURE EFFECT

Special relativity predicts that an object moving with velocity v will experience time moving more slowly. This causes an atom of mass m at temperature T and root mean square velocity $\sqrt{\frac{k_B T}{mc^2}}$ to see an incoming photon slightly redshifted. This causes an apparent shift in the absorption spectrum of the absorber and can be characterized by a temperature coefficient K that relates the

temperature to the shift in energy. This can be calculated by measuring the shift in the absorption peak divided by 14.4 keV over a range of temperatures and calculating the slope of the relative shift versus temperature line.

V. EXPERIMENTAL SETUP

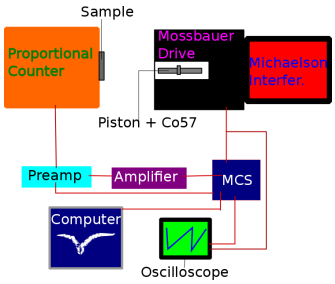

FIG. 2. The experimental setup for this experiment

Figure 2 depicts the experimental arrangement that we used. In essence, we had a Mossbauer drive move a ^{57}Co source according to a sawtooth velocity function. When the ^{57}Co decays, some of the parents will decay into ^{57m}Fe, which will then release a 14.4 keV photon as it falls to its ground state. Since the source is moving, this 14.4 keV photon will be slightly red- or blueshifted, allowing us to probe a small range of energies at a high precision. The proportional counter counts the number of photons that make it past the sample; dips in the output of the proportional counter correspond to absorption peaks in the sample.

V.1. Velocity Calibration

The Michaelson interferometer splits a laser into two beams at 90° angles. One beam remains constant and goes directly to a photodiode while the other beam reflects off of the back of the piston containing the ^{57}Co source. Since the piston is moving, the distance the second beam has to travel will change with time, and the interference of the two beams back at the photodiode will also change. Over the multichannel scalar's (MCS's) dwell time, the interference pattern may go from completely constructive to destructive interference several times. The Michaelson interferometer sends a pulse to be counted by the MCS every time one such cycle completes, and so the number of counts recorded is proportional to the velocity of the piston. Since we are looking at phase shifts of the laser, the constant of proportionality depends on the laser's wavelength λ and tells us that $C_i = NT\left(\frac{2V_i}{\lambda}\right)$, where C_i is the number of counts at channel i, V_i is the corresponding average velocity, N is the number of sweeps done during the calibration, and T is the dwell time of the MCS. Fitting two lines to the velocity curve yielded a mapping between the dwell time

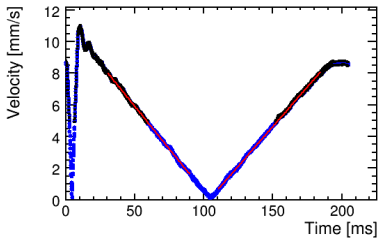

FIG. 3. Two lines fit to the velocity calibration curve with $\chi^2/\text{NDF} = 0.85$ and 0.65, from left to right

and velocity that was used to find our energy shifts. Note that we are actually seeing the absolute value of the velocity, so we had to subtract the velocity predicted by the line on the left in order to actually get velocity. These two lines did not necessarily agree, and so their difference was a major source of error.

VI. RESULTS AND OBSERVATIONS

VI.1. Hyperfine Structures

For this experiment, we put several samples into the Mossbauer spectrometer and recorded their absorption spectra. Figure 4 shows the resultant spectrum for an enriched metallic ^{57}Fe absorber. By fitting six Lorentzians,

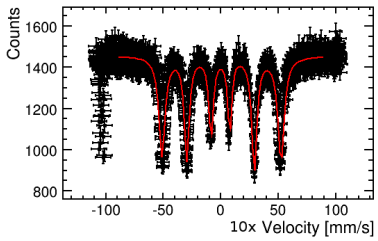

FIG. 4. ^{57}Fe absorption spectrum, showing a complex hyperfine structure

we were able to measure the energy shifts of all of its absorption peaks and calculate several constants regarding its hyperfine structure. These values are all given in table I—note that the ratio $\frac{\mu_0}{\mu_1}$ was obtained by taking the ratio of $\frac{g_0}{g_1}$, since the Zeeman splitting is proportional to the magnetic moments (this is because we assume the magnetic moments align themselves with the magnetic field in iron) and we were able to determine the nuclear magnetic field by using a published value of μ_0. Since the system of equations described above describing the energy shifts is overconstrained, we were able to calculate all of these values in multiple ways to improve our precision and better estimate the random error of our experiment.

We recorded and analyzed the spectra for enriched metallic ^{57}Fe, Fe_2O_3, Fe_3O_4, $FeSO_4$, and $Fe_2(SO_4)_3$. Of note is that the sulfate samples did not demonstrate any

Zeeman shifting—one only showed an isomer shift while the other demonstrated quadrupole splitting as well. We can conclude from this that sulfate atoms do not leave unpaired electrons to create the strong magnetic field the yields Zeeman splitting.

Of particular interest was the Fe_3O_4 sample (magnetite), shown in figure 5. We observed nine separate peaks instead of the ordinary six. This is because the Fe_3O_4 crystal geometry contains tetrahedral and octahedral sites that contain Fe^{2+} and Fe^{3+} ions. At room temperature, these two sites only differ at the lower energy transitions and are therefore degenerate for the three transitions coming from the $m_F = 0\frac{1}{2}$ ground level. However, the $m_F = +\frac{1}{2}$ split into a sites and b sites, as shown in figure 5.

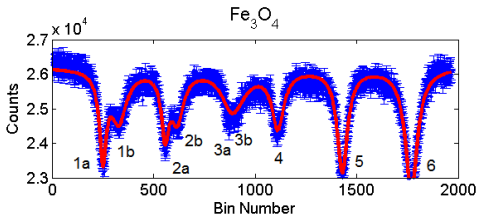

FIG. 5. The absorption spectrum of magnetite, differentiating between a and b lattice sites. χ^2/NDF= 1.34

VI.2. Natural Line Width

We used $Na_3Fe(CN)_6{\cdot}H_2O$ samples of varying thicknesses to determine the natural line width. For this calculation, we followed the procedure outlined earlier and observed a variation shown in figure 6. Extrapolating

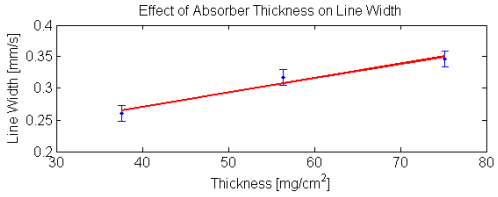

FIG. 6. The thickness versus full width of half maximum to determine the natural line width of ^{57}Fe. χ^2/NDF= 0.82

this data down to zero thickness, we find that ^{57}Fe has a natural line thickness $\Gamma_N = 8.60 \times 10^{-9} \pm 1.34 \times 10^{-9}$ eV. This is within 0.75σ of the accepted value of $9.61e{-}9$ eV[1].

VI.3. Time Dilation and Temperature Coefficient

Using a stainless steel sample at a range of temperatures from 22°C to 115°C, and plotting the energy shift over the lab frame photon energy 14.4 keV ($\frac{\Delta E}{E_0}$), we obtained figure 7. Fitting a line to this curve yields a temperature coefficient $K = -1.9 \pm 0.3 \times 10^{-15}$ °C^{-1}, which is within 0.43σ of the published value $2.09 \pm 0.06 \times 10^{-15}$ °C^{-1}[5].

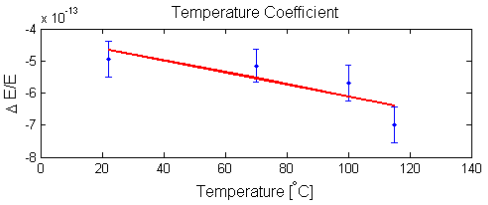

FIG. 7. Temperature versus energy shift for a stainless steel sample. χ^2/NDF=1.27

VII. ERRORS AND CONCLUSIONS

Our measurements of the temperature coefficient and the natural line width both had errors of approximately 16%. Of this, about 3% came from calibration errors. 13% of the line width error and 9% of the temperature coefficient error came from fitting errors (which was largely due to a Poisson error of about 3%, while another 4% of the temperature coefficient error came from variations in the sample temperature. Our hyperfine measurements had errors of roughly 5%, with errors predominantly coming from Poisson errors ($\approx 2.5\%$), calibration errors ($\approx 2\%$), and fitting errors ($\approx 0.3\%$). Errors could have been reduced by using longer integration times.

Overall, we successfully observed relativistic time dilation and measured the temperature coefficient of ^{57}Fe and found its natural line width. We additionally found several measurements of the hyperfine structures of ^{57} in various chemical environments. We were able to use the Mossbauer effect to measure very fine energy scales that would otherwise be impossible to resolve.

[1] "Mossbauer Spectroscopy", MIT Department of Physics, 1/29/09

[2] O.C. Kistner and A.W. Sunyar, Phys. Rev. Lett. 4, 8 (1960)

[3] S. DeBenedetti, G. Lang, and R. Ingalls, Phys. Rev. Lett. 6, 2 (1961)

[4] R. Bauminger, S.G. Cohen, A. Marinov, S. Ofer, and E. Segal, Phys. Rev. 122, 5 (1961)

[5] H. Frauenfelder, The Moessbauer Effect: A Review with a Collection of Reprints, (New York, W.A. Benjamin, Inc.,

1962)

		Value	Accepted	Deviation
^{57}Fe	g_0	$1.81 \pm 0.05 \times 10^{-7}$ eV	1.88×10^{-7} eV	1.4σ
[2]	g_1	$1.06 \pm 0.04 \times 10^{-7}$ eV	1.08×10^{-7} eV	0.5σ
	$\frac{\mu_0}{\mu_1}$	1.71±0.06	1.75	0.67σ
	ϵ	$0\pm3.89 \times 10^{-10}$ eV	0 eV	—
	δ	$0\pm2.88 \times 10^{-9}$ eV	0 eV	—
	B_N	317±9 kOe	330	1.44σ
Fe_2O_3	g_0	$2.85 \pm 0.02 \times 10^{-7}$ eV	$2.93 \pm 0.02 \times 10^{-7}$ eV	3σ
[3]	g_1	$1.68 \pm 0.03 \times 10^{-7}$ eV	$1.66 \pm 0.01 \times 10^{-7}$ eV	0.33σ
	$\frac{\mu_0}{\mu_1}$	1.70±0.06	1.77 ± 0.01	1σ
	ϵ	$2.47\pm0.07 \times 10^{-8}$ eV	$2.26 \pm 0.14 \times 10^{-8}$	1σ
	δ	$1.66\pm0.78 \times 10^{-9}$ eV	$5.8\pm1.4 \times 10^{-9}$ eV	3.5σ
	B_N	500.±7 kOe	513±2 kOe	1.9σ
Fe_3O_4a	g_0	$2.64 \pm 0.03 \times 10^{-7}$ eV	$2.83 \pm 0.10 \times 10^{-7}$ eV	3σ
[4]	g_1	$1.54 \pm 0.07 \times 10^{-7}$ eV	$1.61 \pm 0.07 \times 10^{-7}$ eV	—
	$\frac{\mu_0}{\mu_1}$	1.72±0.08	1.76 ± 0.10	—
	ϵ	$1.93\pm0.4 \times 10^{-8}$ eV	$2.16 \pm 0.05 \times 10^{-8}$	0.45σ
	δ	$0\pm3.61 \times 10^{-9}$ eV	$0\pm0.5 \times 10^{-9}$ eV	—
	B_N	464±15 kOe	500±20 kOe	1.1σ
Fe_3O_4b	g_0	$2.41 \pm 0.06 \times 10^{-7}$ eV	$2.55 \pm 0.10 \times 10^{-7}$ eV	0.67σ
[4]	g_1	$1.47 \pm 0.10 \times 10^{-7}$ eV	$1.49 \pm 0.05 \times 10^{-7}$ eV	—
	$\frac{\mu_0}{\mu_1}$	1.64±0.12	1.76 ± 0.10	0.17σ
	ϵ	$3.43\pm0.40 \times 10^{-8}$ eV	$3.36 \pm 0.05 \times 10^{-8}$	0.1σ
	δ	$0\pm1.2 \times 10^{-8}$ eV	$0\pm0.5 \times 10^{-9}$ eV	—
	B_N	424±23 kOe	450±20 kOe	0.26σ
$FeSO_4$	g_0	0 eV	0 eV	—
[3]	g_1	0 eV	0 eV	—
	$\frac{\mu_0}{\mu_1}$	—	—	—
	ϵ	$5.73 \pm 0.23 \times 10^{-8}$ eV	$6.7 \pm 0.2 \times 10^{-8}$	3.5σ
	δ	$1.46\pm0.01 \times 10^{-7}$ eV	1.5×10^{-7} eV	—
	B_N	0 kOe	0 kOe	—
$Fe_2(SO_4)_3$	g_0	0 eV	0 eV	—
[3]	g_1	0 eV	0 eV	—
	$\frac{\mu_0}{\mu_1}$	—	—	—
	ϵ	$1.76 \pm 0.18 \times 10^{-8}$ eV	$2.6 \pm 0.2 \times 10^{-8}$	2.8σ
	δ	0 eV	0 eV	—
	B_N	0 kOe	0 kOe	—

TABLE I. Values found describing the hyperfine structure of ^{57}Fe in various chemical environments. g_0 and g_1 are the ground state and first excited state Zeeman energy gaps, respectively, $\frac{\mu_0}{\mu_1}$ is the ratio of the magnetic moments of these states, ϵ is the isomer shift, δ is the quadrupole splitting, and B_N is the magnetic field felt by the nucleus.